

Communication and Energy-Aware Multi-UAV Coverage Path Planning for Networked Operations

Mohamed Samshad[✉], and Ketan Rajawat[✉], *Member, IEEE*

Abstract—This paper presents a communication and energy-aware Multi-UAV Coverage Path Planning (mCPP) method for scenarios requiring continuous inter-UAV communication, such as cooperative search and rescue and surveillance missions. Unlike existing mCPP solutions that focus on energy, time, or coverage efficiency, our approach generates coverage paths that require minimal the communication range to maintain inter-UAV connectivity while also optimizing energy consumption. The mCPP problem is formulated as a multi-objective optimization task, aiming to minimize both the communication range requirement and energy consumption. Our approach significantly reduces the communication range needed for maintaining connectivity while ensuring energy efficiency, outperforming state-of-the-art methods. Its effectiveness is validated through simulations on complex and arbitrary shaped regions of interests, including scenarios with no-fly zones. Additionally, real-world experiment demonstrate its high accuracy, achieving 99% consistency between the estimated and actual communication range required during a multi-UAV coverage mission involving three UAVs.

Index Terms—Aerial Systems: Applications, Networked Robots, Path Planning for Multiple Mobile Robots or Agents, Field Robots, Cooperating Robots.

Video: <https://youtu.be/05iLsQy1fpU>

I. INTRODUCTION

In the past few years, the deployment of multiple Unmanned Aerial Vehicles (UAVs) has attracted the interest of many enterprise fields, becoming a powerful tool for professionals to acquire data in a fast and efficient way. Multi-UAV systems have revolutionized various industries by enabling complex missions to be carried out quickly and with precisely, making them invaluable in fields such as surveillance [1], photogrammetry [2], agricultural monitoring, precision farming [3], and Search And Rescue (SAR) [4], [5]. By utilizing multiple UAVs simultaneously, entire regions of interest can be surveyed quickly and thoroughly, addressing challenges that were previously difficult to overcome.

The advantages of multi-UAV systems are evident in their ability to rapidly cover large areas and coordinate tasks seamlessly. They efficiently scan vast regions for SAR operations, monitor crop health and manage resources in agriculture [6], [7], and assess disaster-stricken areas by generating detailed maps and 3D models for informed decision-making [8]. These capabilities showcase the transformative impact of multi-UAV systems across diverse sectors, driving innovation and enhancing operational efficiency.

Given the diverse applications of multi-UAV systems, efficient and safe path planning is crucial for executing coordinated missions. A major challenge in Multi-UAV Coverage

Path Planning (mCPP) is generating paths that maximize coverage within the Region of Interest (ROI), minimize energy consumption, and maintain communication throughout the mission. Optimizing all of these factors is an NP-hard problem. Although various solutions have been proposed, they include algorithms that handle No-Fly Zones (NFZs) [9]–[11], enhance energy efficiency [10], [12], optimize flight speed [10], and support uneven load distribution [9], [12].

While research on mCPP has predominantly focused on optimizing energy, coverage, and time, the consideration of communication requirements in coverage path planning remains largely unexplored. In multi-UAV cooperative missions, reliable communication between vehicles is crucial. Designing coverage paths without accounting for communication needs can lead to frequent disconnections during the mission. This can result in coordination challenges and potential data loss. Maintaining reliable communication is especially critical in operations such as security surveillance, inspection, and SAR, where it is essential for mission success.

In this paper, we propose a communication and energy aware mCPP algorithm that generates coverage paths with minimal inter-UAV communication range requirements. This ensures that all UAVs remain connected throughout the mission in a mesh network architecture. Simultaneously, the algorithm minimizes energy consumption, maximizes area coverage, and completes the mission efficiently. The algorithm utilizes the groundwork laid by Divide Areas based on Robots Initial Positions (DARP) algorithm [9], solving the mCPP problem through area discretization with optimal allocation and constructing a Spanning Tree Coverage(STC) paths on polygonal regions. Energy consumption for the coverage paths is estimated using a direct power consumption model based on the UAVs' physical parameters.

The primary contribution of this paper is an optimization algorithm that generates coverage paths with minimal inter-UAV communication range requirements. We achieve this by treating the range requirement and energy consumption as hyperparameters in the optimization process, solved using Bayesian optimization techniques across multiple DARP initialization trials. Additionally, we optimize the starting points on generated paths to further minimize communication range requirements. A time-sampling methodology is implemented on these paths, followed by continuous connectivity evaluation to analyze range needs. An optimal shift and rotation technique is applied before discretizing the polygon into cells, enhancing coverage efficiency. This multi-layered optimization framework improves inter-UAV connectivity and energy efficiency, while also supporting complex polygons with NFZs.

II. RELATED WORK

Coverage Path Planning (CPP) is a well-addressed problem, with several solutions already implemented in real-world path planning applications such as floor-cleaning robots, painting systems, UAV survey path planners, and agricultural spraying robots [13]–[15]. This section discusses some of the works that have provided key motivation for this paper through their innovative approaches to the problem or optimized results for different flight parameters.

Among the key studies, Comprehensive analyses of CPP techniques are provided in [16], [17], where the authors explore a range of bio-inspired, computational, and analytical CPP methodologies. These studies offer valuable insights into area division and path-planning algorithms for both simple and complex ROIs. They address CPP challenges in both 2D and 3D environments, with and without no-fly zones, primarily focusing on single-robot applications while also considering multi-robot path planning. The use of boustrophedon cell division [17], STC [9], and energy-aware CPP strategies [?] are highlighted, with emphasis on optimizing flight parameters such as energy consumption, path length, and coverage efficiency. These analyses underscore the complexities of CPP, particularly in cooperative multi-robot scenarios.

Another notable contribution is the introduction of boustrophedon cell decomposition as an alternative to classical trapezoidal decomposition [11], [18]. This technique enables CPP in ROIs with no fly zone by partitioning them into cells and using systematic back-and-forth sweeping paths within each cell. A graph traversal method is then used to connect these individual paths into a complete coverage path. Building on this, [19] revisits boustrophedon CPP by replacing the graph traversal method with the Generalized Traveling Salesman Problem (GTSP) [20] to determine the optimal path configuration, minimizing time and directional changes and improving energy efficiency.

While these studies present foundational CPP algorithms, many proposed solutions are optimized for various flight parameters, focusing on minimizing flight path length [10], [21], [22], mission time [19], the number of path turns [12], [23], [24], energy consumption along the path [10], [12], and inter-UAV connectivity [25]. A recent study introduces an Energy-Aware mCPP (EA-mCPP) strategy specifically for multi-UAV operations, focusing on optimizing energy consumption and flight speed [10]. This approach uses an accurate energy model [26] to predict expenditure across boustrophedon cells and calculate optimal flight speeds. The method employs the Multiple Set Traveling Salesman Problem (MS-TSP) [27] to determine energy-efficient routing, ensuring effective resource allocation and path utilization in UAV missions.

All of the discussed CPP solutions utilize area partitioning and optimal allocation. In [25], a formation flying technique was proposed for multi-UAV coverage missions in ROIs without any NFZs. This approach ensures that the inter-UAV distance remains within the range due to the rigid formation shape, thereby maintaining the UAVs within communication range of each other. Another distinct technique involves discretizing the ROI into grid cells and performing STC. In

TABLE I: Qualitative Comparison of the Related Methods

	Comm. aware	Energy aware	Energy efficient	Custom load dist.	No fly zones
Proposed	✓	✓	✗	✓	✓
Cooperative cpp [21]	✗	✗	✓	✓	✓
EA-mCPP cpp [10]	✗	✓	✓	✗	✓
DARP+MST [9]	✗	✗	✗	✓	✓
O-DARP [12]	✗	✗	✓	✓	✓
POPCORN+SALT [28]	✗	✗	✓	✓	✗
Formation flying [25]	✓	✗	✓	✗	✗

[9], a fast and effective algorithm is proposed by discretizing the ROI into square grid cells and then using a modified Voronoi algorithm to allocate cells to each robot. The STC algorithm [29] is then implemented for each region to generate independent coverage paths. A similar approach is used in [30], where adaptive grid size discretization and the optimal allocation minimum spanning tree are employed to generate smooth and minimal-cost paths.

To optimize energy in DARP-generated paths, [12] proposes the use of machine learning techniques for generating energy-efficient coverage paths. In this approach, the energy consumption of paths is mapped to the number of turns, and optimization techniques are applied to generate paths with fewer turns across different DARP initialization.

In contrast to the works discussed above, while all of the proposed approaches present interesting ideas to reduce flight time and energy consumption, they also exhibit several limitations. For instance, many approaches fail to handle arbitrary or complex ROIs, particularly those with NFZs, and do not account for communication constraints that are critical in cooperative missions. Moreover, some methods, like the formation flying technique proposed in [25], focus solely on maintaining inter-UAV distance under range but cannot work for ROIs with NFZs. A comparison of the discussed approaches is summarized in Table I.

III. PROBLEM FORMULATION

Consider a ROI defined as a 2D polygonal area that needs to be fully scanned by a group of N UAVs. Every point within the ROI must be observed at least once using the UAV’s sensor during the mission. The ROI may contain No-Fly Zones (NFZs), which are areas that UAVs must avoid. The primary objective of this UAV group is to work collaboratively to achieve complete coverage of the ROI while maintaining continuous connectivity within a UAV mesh network [31]. Each UAV must be able to communicate with all other UAVs at all times, either directly or through multi-hop communication.

Our goal is to generate multi-UAV coverage paths that ensure continuous inter-UAV communication, minimize energy consumption, maximize coverage efficiency, and avoid entering NFZs. The proposed communication and energy-aware mCPP algorithm is described at a high level in Section III-A. Section III-B explains the representation of the ROI on a grid, while Section III-C discusses the connectivity assessment in the coverage paths. The techniques used for estimating energy consumption are outlined in Section III-D, and Section III-E describes the iterative optimization process

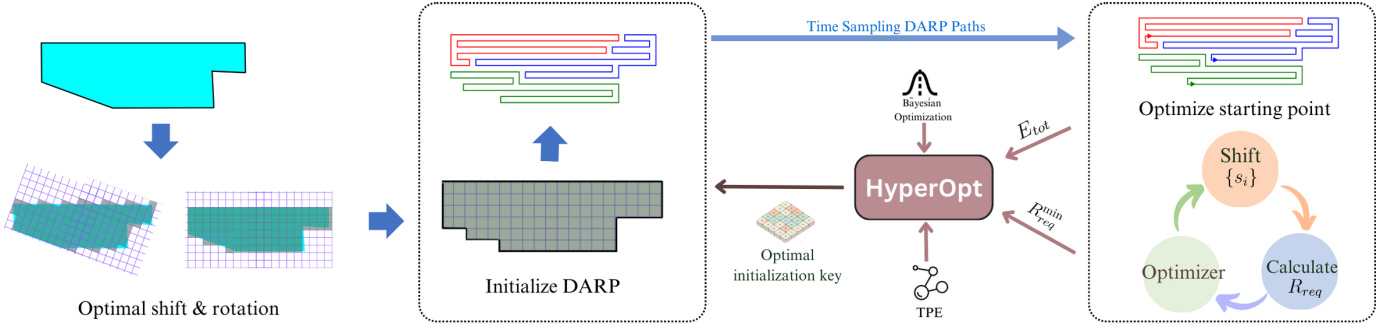


Fig. 1: Optimization process breakdown: ROI Discretization through optimal shifts and rotation, DARP-MST path generation, time-sampling & energy calculation, start point optimization by connectivity analysis, hyper parameter optimization with range and energy for next DARP initialization

Algorithm 1: Communication and energy aware mCPP

Input: ROI, N , λ , UAV_{param} , \mathcal{G} , \mathcal{O}

Output: Best Paths (P_{best})

```

1  $R^* \leftarrow +\infty$  // Best range requirement;
2  $E_{tot}^* \leftarrow +\infty$  // Total energy for  $P_{best}$ ;
3  $f^* \leftarrow +\infty$  // Objective function;
4  $P_{best} \leftarrow \{\}$ 
5 Process ROI to grid cells and NFZs;
6 Optimize grid alignment via shifts and rotations;
7 Optimization:
8   foreach trial in  $N_{darp}$  do
9     Generate DARP initialisation keys;
10    Generate DARP paths;
11    Time-sample paths using  $s_f^{u_i}$ ,  $s_t^{u_i}$ , and  $r_t^{u_i}$ ;
12    Optimizing starting positions:
13    foreach trial in  $N_{shift}$  do
14      Shift start position & compute  $R_{req}$ ;
15      Minimize  $R_{req}$  via optimal shifts;
16      Return optimal paths ( $p$ )
17    Compute  $E_{tot}$  and  $R_{req}^{min}$  for each set of paths;
18    Compute object. function  $f_o = R_{req}^{min} + \lambda \cdot E_{tot}$ ;
19    if  $f < f^*$  then
20      Update  $f^* \leftarrow f$ ;
21      Update  $R^* \leftarrow R_{req}^{min}$ ;
22      Update  $E_{tot}^* \leftarrow E_{tot}$ ;
23      Update  $P_{best} \leftarrow p$ ;
24    Update optimization model with results;

```

that identifies communication and energy-aware mCPP paths. For applications with short communication ranges, Section III-F proposes formation flying as a special case. Finally, Section III-G outlines the operational constraints and assumptions made during this work.

A. Communication and energy aware mCPP Algorithm

The proposed communication and energy-aware mCPP algorithm generates flight paths for N UAVs ($N \geq 2$) that maximize ROI coverage while maintaining continuous connectivity within the UAV mesh network. The method introduces a parameter $\lambda \in [0, \infty)$ to trade off between

minimizing communication range and energy consumption. Setting $\lambda = 0$ prioritizes minimizing communication range only, while higher values prioritize energy efficiency.

The algorithm requires inputs such as UAV_{param} : UAV parameters (e.g., turning radius, speed profile), \mathcal{G} : grid parameters (e.g., cell size, coverage threshold), and \mathcal{O} : optimization parameters (e.g., number of trials, optimization time). Algorithm 1 summarizes the process, which begins by discretizing the ROI into grid cells and incorporating NFZs. An optimal shift and rotation process adjusts the grid's alignment and orientation to maximize ROI coverage, minimize energy consumption, and enable precise path planning [21].

The optimization process starts by generating DARP paths using random initialization on a 2D grid [9]. The objective function f_o is evaluated for each path using (7), considering communication range and energy consumption.

The algorithm performs N_{darp} optimization trials to identify effective DARP initializations, aiming to minimize f_o for each path. The closed-loop structure of DARP paths allows for optimizing the mission starting point, further minimizing the communication range requirement.

A secondary optimization process with N_{shift} trials adjusts UAVs' starting positions to minimize the communication range (R_{req}) for maintaining connectivity. The minimum required range, R_{req}^{min} , is determined using (4).

After generating paths and identifying optimal starting positions, total energy consumption (E_{tot}) is estimated (Section III-D), and f_o is computed using (7). If a trial yields a lower f_o , the optimal paths (P_{best}) and metrics are updated.

The iterative process continues for N_{darp} trials, outputting UAV paths that balance communication reliability and energy efficiency based on the specified λ value. Fig. 1 illustrates the optimization process.

B. ROI and NFZ Representation on grid, Area division and Path planning

In mCPP, various methods have been proposed for area division and path planning. Conventional approaches, such as Trapezoidal and Boustrophedon decomposition, divide the ROI into sub-regions for each robot to cover. However, these methods have several limitations. They often result in an unbalanced distribution of coverage areas among the robots,

which can lead to inefficient resource utilization. Moreover, these methods typically divide areas into simple polygonal shapes that not suited for maintaining connectivity during coverage, especially in arbitrary and complex ROIs.

To address these limitations, we propose using the DARP algorithm [9] for area division and path planning. DARP excels in dividing arbitrary and complex ROIs into intertwined sub-regions while maintaining a balanced area distribution among the robots. The intertwined area structure, combined with the iterative optimization of DARP initialization, helps generate sub-regions that are suited for connected coverage. The STC path planning algorithm [29] is then employed to generate closed-loop paths for covering the divided sub-regions.

ROI representation: The ROI is discretized into equal-sized square grid cells based on a specified path width. The cell side length is set to twice the parallel distance between paths, as required by the STC path generation algorithm. A coverage threshold $\tau \in [0, 1]$ is applied to determine the inclusion of border cells in the ROI representation. Only cells meeting or exceeding this threshold are considered part of the ROI. For instance, $\tau = 0.1$ includes border cells with at least 10% of their area inside the ROI, while $\tau = 1.0$ requires cells to be entirely within the ROI, potentially reducing coverage efficiency. This same thresholding technique is applied to identify NFZs, ensuring accurate representation within the grid. To optimize coverage, we perform a shift and rotation operation that maximizes the number of cells meeting the coverage threshold, following the method detailed in [21]. The goal of this adjustment is twofold: (1) to reduce the number of partially covered cells at the edges of the ROI, thereby maximizing the usable coverage area, and (2) to minimize redundant overlaps, which can waste energy.

Area division and path planning: The DARP algorithm is employed for area division, and it utilizes the STC path planning algorithm, taking the discretized grid representation of the ROI as input. DARP divides the grid into exclusive sub-regions for each UAV to cover through a modified Voronoi partitioning, where grid cells are assigned to the nearest UAV based on initial positions. This process ensures the distribution of coverage areas among the UAVs according to the required ratio. The algorithm iteratively adjusts the boundaries between sub-regions to achieve the desired area distribution, resulting in a set of non-overlapping, connected sub-regions. Subsequently, the STC path planning algorithm is applied to generate closed loop coverage path for each sub region.

C. Connectivity Assessment in Multi-UAV Paths

Time-sampling: The position of the i^{th} UAV on the path at time t , denoted as $P_t^{u_i}$, is estimated through the time-sampling process shown in (1). This estimation is based on the speed parameters of each UAV, such as forward speed ($s_f^{u_i}$), turning speed ($s_t^{u_i}$), and turning radius ($r_t^{u_i}$). The individual time-sampling process allows each UAV to operate with distinct speed configurations, accommodating varying mission requirements and vehicle capabilities.

$$P_t^{u_i} = f\left(s_f^{u_i}, s_t^{u_i}, r_t^{u_i}\right) \quad (1)$$

Algorithm 2: Optimize launch points for connectivity

Input: Time-Sampled Paths, N_{shift} , Step size (s_{step})
Output: Best shift combination ($\{\Delta s_i\}_{best}$), Minimum required distance (R_{req}^{min})

```

1  $\{\Delta s_i\}_{best} \leftarrow \{\}; R_{req}^{min} \leftarrow +\infty;$ 
2 Optimization:
3   foreach  $trial$  in  $N_{shift}$  do
4     Generate shifts  $\{\Delta s_i\}$  and apply to paths;
5      $R_{req} \leftarrow \max_{t \in T} (R_{req}(t, \{\Delta s_i\}));$ 
6     if  $R_{req} < R_{req}^{min}$  then
7        $R_{req}^{min} \leftarrow R_{req}; \{\Delta s_i\}_{best} \leftarrow \{\Delta s_i\};$ 

```

Result: Return $\{\Delta s_i\}_{best}$ and R_{req}^{min}

Connectivity analysis: At any given time instance t , the required communication range $R_{req}(t)$ is the minimum distance r that ensures all UAVs, with positions $P_t^{u_i}$, remain connected in a mesh network, as shown in (2). The overall range requirement R_{req} for maintaining connectivity throughout the entire mission is then determined by finding the maximum communication range needed across all time instances $t \leq T$, where T represents the total mission time, as expressed in (3).

$$R_{req}(t) = \min\{r : \{P_t^{u_i}\} \text{ form a mesh with range } r\} \quad (2)$$

$$R_{req} = \max_{t \leq T} (R_{req}(t)) \quad (3)$$

Optimizing launch point: The initial R_{req} is calculated using the default starting point combination s_0 . Due to the closed-loop nature of the generated paths, starting points can be shifted by Δs_i in various combinations inside the path, each altering R_{req} . Finding the optimal starting point in this large set of combinations is computationally expensive and time-consuming. A probabilistic model-based optimization is particularly suited for this task, it efficiently explores the combination space by balancing exploration and exploitation. The high-level overview of this process is shown in Algorithm 2. Bayesian optimization is implemented over N_{shift} trials to identify the starting point combination that minimizes R_{req} , as expressed in (4). This approach systematically finds the optimal starting points without exhaustively searching all combinations. The resulting R_{req}^{min} is then used to calculate the objective function f_o .

$$R_{req}^{min} = \min_{\{\Delta s_i\}} \left(\max_t (R_{req}(t, \{\Delta s_i\})) \right) \quad (4)$$

D. Estimating Energy Consumption for Paths

Estimating the energy consumption of UAV flight paths can be performed using various methods, depending on the desired accuracy level. For instance, in [26], the authors present a method that calculates UAV energy consumption based on comprehensive UAV parameterization. Alternatively, [?] describes an approach that estimates energy consumption by generating trajectories of the flight path.

While these methods provide accurate energy consumption estimates, they often require detailed UAV parameters or complex trajectory generation processes. In our work, we

prioritize a more lightweight and computationally efficient approach that can be easily integrated into the optimization process without compromising the overall accuracy of the energy consumption estimates.

To achieve this, we propose a method for estimating energy consumption based on analyzing the path waypoints, power consumption model, and speed parameters of the mission. This approach allows us to capture the essential factors influencing energy consumption while maintaining a simple and efficient calculation process. our power consumption model is defined as follows:

$$P(v) = P_b + P_d(s) \quad (5)$$

Where:

- P_b : power required to run electronics, sensors, and communication systems.
- $P_d(s)$: power required to overcome air resistance while moving with speed s , calculated separately for straight paths and turns

Path segmentation and energy estimation: Each UAV path is divided into straight-line and turning segments by considering the turning radius at each corner waypoint. This segmentation helps identify the total time spent on straight-line movements (ΔT_{s_f}) and turning maneuvers (ΔT_{s_t}). For each path, we calculate the energy consumption using the UAV's empirically derived power model, which distinguishes between forward flight ($P_d(s_f)$) and turning ($P_d(s_t)$) power requirements. The total energy consumption for a path is then calculated as:

$$E_{\text{path}} = P_b \cdot T + P_d(s_f) \cdot \Delta T_{s_f} + P_d(s_t) \cdot \Delta T_{s_t} \quad (6)$$

DARP paths consistently produce rectangular turns, which allows us to assume uniform energy consumption for all turns. This characteristic simplifies the energy estimation process, enabling our algorithm to rapidly calculate the energy requirements for each UAV path using the power consumption model. The total energy requirement for the entire mission is then determined by summing the energy consumption of each individual path. This streamlined approach, enables the efficient evaluation of numerous potential paths while maintaining adequate accuracy for comparative assessment.

E. Optimization Problem

The optimization problem involves finding the optimal DARP initialization positions for each UAV on a 2D grid that minimize both the required communication range and energy consumption. Given a grid with C cells and N UAVs, the search space size is C^N , growing exponentially and making exhaustive search computationally infeasible. Therefore, we employ Bayesian optimization, specifically the Tree-Structured Parzen Estimator (TPE) algorithm implemented within the Optuna framework, to efficiently explore this vast search space. TPE builds probability models of the objective function values conditioned on hyperparameter configurations and uses them to determine the most promising areas to sample. The objective function f_o is defined as:

$$f_o = R_{req}^{min} + \lambda \cdot E_{tot} \quad (7)$$

where R_{req}^{min} is the minimum required communication range throughout the mission (in meters), E_{tot} is the total estimated energy consumption (in watt-hours), and λ is the user-defined trade-off coefficient. The optimization is subject to constraints of complete area coverage and avoidance of NFZs. Optuna's implementation allows for efficient parallel computing and dynamic pruning of unpromising trials, significantly speeding up the optimization process. Here, an 'unpromising trial' is defined as one whose objective function value is significantly worse than the current best, allowing early termination to save computational resources.

Decision variables: Key variables influence the optimization process:

- *Startup Trials:* Initial random trials build a model of the search space, providing a baseline for Bayesian optimization. We use 20% of the total trials as startup trials to establish this baseline.
- *Pruning Mechanism:* A median pruner is used to terminate unpromising trials early. If a trial's intermediate objective value is worse than the median of previous trials' values at the same step, it is pruned.
- *$N_{ei_candidates}$:* Controls the number of candidates sampled in each TPE iteration, balancing thorough exploration with computation time. This choice impacts the trade-off between exploration and exploitation.

F. Special Case: Formation Flying

Formation flying becomes essential when the inter-UAV communication range is significantly limited (3-5 times the path width). However, the rigid nature of formation shapes makes it challenging to implement in complex ROIs, particularly those with NFZs. A basic model of the formation flying strategy for large-area coverage is discussed in [25], but it lacks consideration for formation shape changes during turns and is not optimized for energy efficiency. For large areas within regular polygonal ROIs and scenarios with strict communication constraints, we propose a communication-aware formation path generation method, as outlined in Algorithm 3. In this approach, the combined formation footprint F_c is calculated by summing the widths of individual UAV footprints and treated as a single footprint for generating STC path. Offset paths are then created for individual UAVs with parallel spacing corresponding to their respective footprints, followed by a connectivity assessment performed after time sampling and starting point optimization.

G. Operational Constraints and Assumptions

The following assumptions and constraints were applied in the experiment:

- 1) *Uniform UAV Parameters:* All UAVs have identical communication range and communicating with a mesh architecture.
- 2) *Calculated Starting Points:* UAVs begin their mission from pre-determined starting points only. They all start the mission simultaneously.
- 3) *Exclusion of Takeoff and Landing:* The energy for takeoff and landing phases is excluded from the calculations, focusing solely on the mission's operational phase.

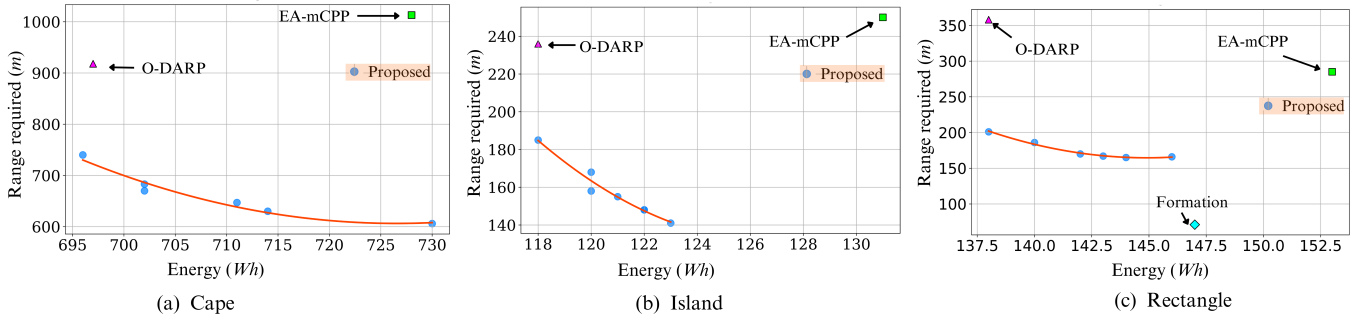


Fig. 2: Performance comparison of the proposed algorithm versus state-of-the-art methods across various ROIs

Algorithm 3: Formation Path Planning

Input: ROI, N , Sensor footprints F_{u_i}

Output: Optimized formation paths P_{u_i} for each UAV

- 1 Discretize ROI into grid cells;
 - 2 Align grid via shifts and rotations;
 - 3 **Generate Combined Coverage Path**
 - 4 Calculate formation width: $F_c = \sum_{i=1}^N F_{u_i}$;
 - 5 Generate single STC path P_c for F_c ;
 - 6 **Generate Individual UAV Paths**
 - 7 **foreach** UAV i from 1 to N **do**
 - 8 Create offset paths P_{u_i} parallel to P_c ;
 - 9 Time-sample all paths using $s_f^{u_i}$ & $s_t^{u_i}$;
 - 10 **Optimize Starting Positions**
 - 11 **foreach** trial in N_{shift} **do**
 - 12 Adjust start position and compute R_{req} ;
 - 13 Minimize R_{req} with optimal shifts;
 - 14 **Result:** Save optimized paths P_{u_i} ;
-

IV. EVALUATION RESULTS

To evaluate the effectiveness of the proposed approach, we first conducted simulations using the ArduPilot Software-in-the-Loop (SITL) simulator. After confirming its performance in the simulated environment, we carried out real-world tests with three UAVs to assess the method's real-world accuracy and performance. For benchmarking purposes, we compared our approach with three state-of-the-art methods within the SITL environment, as illustrated in Fig. 2. To the best of our knowledge, our method is the first to generate communication-aware coverage paths for arbitrarily shaped ROIs, including support for NFZs, while also allowing users to balance energy consumption and communication requirements in the optimization process. In contrast, existing methods primarily focus on minimizing energy consumption, either directly or through related metrics. To ensure accurate energy estimation, we developed a power consumption model from real-world experiments with our UAVs, which was then applied to the simulations to closely reflect actual operational conditions.

A. Hardware Specifications and Flight Metrics

All simulations were conducted on a computer equipped with a 12th Gen Intel(R) Core(TM) i7-12700K CPU, 32GB RAM, and running Ubuntu 20.04.6 LTS OS. For the experiments, we used a custom-built quadcopter platform, featuring

a Raspberry Pi4B as the onboard computer and a Ubiquity Bullet M2 [32] with OpenWRT firmware for wireless mesh networking. The UAV operated at a forward flight speed of 5 m/s, a turning speed of 3 m/s, and a mission altitude of 30 m above ground level. Time-stamped waypoint paths were used to synchronize the relative positions of the UAVs throughout the mission. The basic power consumption P_b was calculated as 5W, with additional power requirements of $P_{drag}(s_f) = 505W \pm 10W$ for forward speed and $P_{drag}(s_t) = 498W \pm 8W$ for turning speed. All optimization operations were performed with 3000 DARP trials (N_{darp}) and 1000 shift trials (N_{shift}). With the given computer specifications, these optimizations took approximately 60 minutes to complete.

B. Validation in Simulation

The performance of the proposed method was evaluated and compared with existing communication and energy-aware approaches in simulations using three UAVs. The comparison included three existing implementations: EA-mCPP [10], the O-DARP approach [12], and a formation flying strategy [25]. The test scenarios applied to each ROI were:

- *Cape*: An ROI used in [28], with the same parameters (35 m coverage footprint) and an area of 903,300 m².
- *Island*: A semi-circular shape with a 15 m coverage footprint and an area of 71,000 m².
- *Rectangle*: A rectangular ROI with a 15 m coverage footprint and an area of 77,000 m².
- *Simple*: A simple polygonal shape with a 15 m coverage footprint and an area of 71,000 m².
- *Complex*: A complex shape with a 15 m coverage footprint and an area of 105,000 m².
- *Island with NFZ*: An island shape with an NFZ, a 15 m coverage footprint, and an area of 70,000 m².

The visual representation of five of the generated paths is shown in Fig. 3. Additionally, the connectivity estimation for complex and island ROIs with NFZs is explained in the supplementary video. Fig. 2 presents the simulation results of the proposed solution across cape, island, and rectangular-shaped regions of interest (ROIs), with varying energy-communication trade-off coefficients (λ). Analyzing the impact of λ across different ROIs shows that while the most energy-efficient coverage paths require a larger connectivity range, the most connected paths are not always the most energy-efficient.

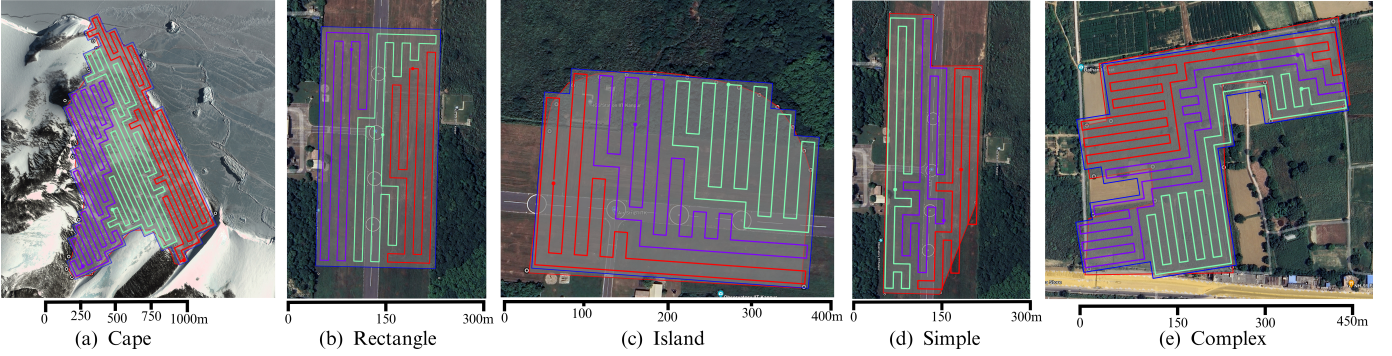


Fig. 3: Scenarios used for experimental evaluation of the proposed method. Shade-of-grey polygons represent arbitrary ROI, and blue polygon is the processed ROI.

In Fig. 2, the Pareto front is marked in orange, indicating the optimal values tuned for different levels of energy and communication awareness. The energy and communication requirements of the energy-aware mCPP (EA-mCPP) method [10] are shown with a green rectangle mark, while the requirements of the optimal DARP (O-DARP) algorithm [12] are indicated with a purple triangle mark. The performance of the formation flying strategy [25] is compared in the rectangular ROI in Fig. 2(c).

After comparing the performance across different ROIs, the results indicate that our method consistently reduces the communication range requirement to 60% of what is needed by the existing O-DARP and EA-mCPP methods. Although formation flying is the only existing communication-efficient mCPP technique, it fails to account for energy efficiency. Furthermore, the major limitation of formation flying lies in its dependency on the shape of the ROI and the presence of NFZs. This comprehensive analysis underscores the importance of balancing both energy and communication considerations to achieve optimal performance in multi-UAV coverage path planning.

C. Real World Experiments

To validate the feasibility of the proposed method in real-world scenarios and assess the accuracy of the simulation, we conducted two types of experiments, as discussed in Section IV-A. The first experiment focused on analyzing the power consumption model of the UAV at different phases of the mission. Next, the accuracy of the range requirement calculation and energy estimation technique was verified by performing a multi-UAV cooperative coverage mission with three UAVs under the specified flying conditions. The mission was conducted over the simple polygon ROI shown in Fig. 3(d), with a coverage area of 71,000 m².

The connectivity strength along the path is shown in a heat map in Fig. 4. Blue arrows mark the vehicles' starting positions, with strong connections in green and weak connections in red. This visualization helps identify potential weak spots in the network, allowing for mitigation of connectivity issues and enabling more effective data exchange planning.

The communication range requirements and mission duration from the real-world experiment were compared with the

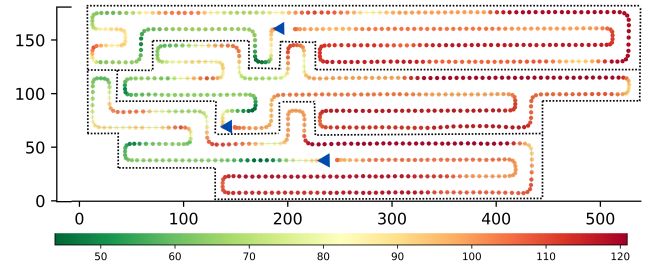


Fig. 4: Connectivity strength along UAV paths

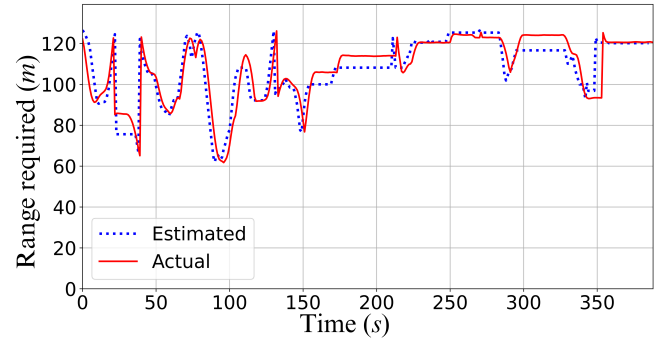


Fig. 5: Range requirement vs Time

estimated results, as shown in Fig. 5. The estimated minimum range requirement was 125.3 meters, while the real-world experiment showed a slightly lower range requirement of 124.21 meters. This minor difference between the estimated and actual paths is due to the fact that in real-world situations, UAVs take curved turns at corners instead of sharp rectangular turns. Similarly, the estimated mission duration was 385 seconds, but the actual mission took 389 seconds. This 4-second difference in mission time is attributed to a small error in the turning speed profile of the estimated and actual drones. In the estimation, we did not consider the acceleration or deceleration for switching between forward speed and turning speed. However, actual UAVs have an acceleration model, which introduces a small error of about 150ms during each turn. This error accumulates to 4 seconds over the entire mission.

The real-world experiment demonstrates that the proposed estimation method achieves 99.9% accuracy in determining

the minimum range requirement for the mission (Fig. 5). Minor deviations between the estimated and actual range requirements occur during specific time intervals (155-210s and 300-330s) due to the delay in UAV paths resulting from differences in turning speed, which causes a variation in the relative positions of the UAVs compared to the estimated positions. The difference in energy consumption was small, with the estimation predicting 130.44 kW and the actual energy consumption being 136.10 kW, resulting in a 95.8% accuracy. This discrepancy is primarily due to approximation techniques and external environmental influences.

V. CONCLUSION

We proposed a novel communication and energy-aware multi-UAV coverage path planning method based on area discretization and Minimum Spanning Tree (MST) generation. To the best of our knowledge, this is the first solution that generates communication-aware paths for inter-UAV cooperative missions requiring continuous communication. By introducing the communication-energy coefficient in the optimization process, our method uniquely allows users to adjust the trade-off between energy awareness and communication awareness during path generation. We compared our approach to state-of-the-art methods through a series of simulation experiments, where it outperformed them in most cases, reducing communication range requirements by 20-60%. Additionally, our solution demonstrated superior energy awareness compared to existing communication-aware methods. The feasibility of the method was also validated in simulations for arbitrary polygonal shapes and polygons with no-fly zones. Furthermore, we verified the effectiveness of the proposed method in real-world scenarios using a set of three UAVs.

REFERENCES

- [1] N. Nigam, "The multiple unmanned air vehicle persistent surveillance problem: A review," *Machines*, vol. 2, no. 1, pp. 13–72, 2014.
- [2] X. Zheng, F. Wang, and Z. Li, "A multi-UAV cooperative route planning methodology for 3D fine-resolution building model reconstruction," *ISPRS Journal of Photogrammetry and Remote Sensing*, vol. 146, pp. 483–494, 2018.
- [3] A. Basiri, V. Mariani, G. Silano, M. Aatif, L. Iannelli, and L. Glielmo, "A survey on the application of path-planning algorithms for multi-rotor UAVs in precision agriculture," *The Journal of Navigation*, vol. 75, no. 2, pp. 364–383, 2022.
- [4] J. Scherer, S. Yahyanejad, S. Hayat, E. Yanmaz, T. Andre, A. Khan, V. Vukadinovic, C. Bettstetter, H. Hellwagner, and B. Rinner, "An autonomous multi-UAV system for search and rescue," in *Proc. First Workshop on Micro Aerial Vehicle Networks, Systems, and Applications for Civilian Use*, 2015, pp. 33–38.
- [5] E. T. Alotaibi, S. S. Alqefari, and A. Koubaa, "LSAR: Multi-UAV collaboration for search and rescue missions," *IEEE Access*, vol. 7, pp. 55 817–55 832, 2019.
- [6] H. S. Lee, B. S. Shin, J. A. Thomasson, T. Wang, Z. Zhang, and X. Han, "Development of multiple UAV collaborative driving systems for improving field phenotyping," *Sensors*, vol. 22, no. 4, p. 1423, 2022.
- [7] L. Fabianto, M. K. D. Hardhienata, and K. Priandana, "Multi-UAV coordination for crop field surveillance and fertilization," in *Proc. 2020 International Conference on Computer Science and Its Application in Agriculture*, 2020, pp. 1–6.
- [8] N. M. Noor, A. Abdullah, and M. Hashim, "Remote sensing UAV/drones and its applications for urban areas: A review," in *IOP Conference Series*, vol. 169, 2018, p. 012003.
- [9] A. C. Kapoutsis, S. A. Chatzichristofis, and E. B. Kosmatopoulos, "DARP: Divide areas algorithm for optimal multi-robot coverage path planning," *Journal of Intelligent & Robotic Systems*, vol. 86, pp. 663–680, 2017.
- [10] D. Datsko, F. Nekovar, and R. Penicka, "Energy-aware multi-UAV coverage mission planning with optimal speed of flight," *IEEE Robotics and Automation Letters*, 2024.
- [11] H. Choset and P. Pignon, "Coverage path planning: The boustrophedon cellular decomposition," in *Field and Service Robotics*, 1998, pp. 203–209.
- [12] A. Stefanopoulou, E. K. Raptis, S. D. Apostolidis, S. Gkelios, A. C. Kapoutsis, S. A. Chatzichristofis, S. Vrochidis, and E. B. Kosmatopoulos, "Improving time and energy efficiency in multi-UAV coverage operations by optimizing the UAVs' initial positions," *International Journal of Intelligent Robotics and Applications*, pp. 1–19, 2024.
- [13] ArduPilot Development Team, "Mission planner flight plan," <https://ardupilot.org/planner/docs/mission-planner-flight-plan.html>, accessed: Aug. 13, 2024.
- [14] "iRobot Website," <http://www.irobot.com>, accessed: Aug. 13, 2024.
- [15] "DJI Flight Planner Website," <https://www.djiflightplanner.com/>, accessed: Aug. 13, 2024.
- [16] E. Galceran and M. Carreras, "A survey on coverage path planning for robotics," *Robotics and Autonomous Systems*, vol. 61, no. 12, pp. 1258–1276, 2013.
- [17] T. M. Cabreira, L. B. Brisolara, and P. R. Ferreira Jr, "Survey on coverage path planning with unmanned aerial vehicles," *Drones*, vol. 3, no. 1, p. 4, 2019.
- [18] R. Seidel, "A simple and fast incremental randomized algorithm for computing trapezoidal decompositions and for triangulating polygons," *Computational Geometry*, vol. 1, no. 1, pp. 51–64, 1991.
- [19] R. Bähnamann, N. Lawrance, J. J. Chung, M. Pantic, R. Siegwart, and J. Nieto, "Revisiting boustrophedon coverage path planning as a generalized traveling salesman problem," in *Field and Service Robotics: Results of the 12th International Conference*, 2021, pp. 277–290.
- [20] M. Fischetti, J. J. Salazar González, and P. Toth, "The symmetric generalized traveling salesman polytope," *Networks*, vol. 26, no. 2, pp. 113–123, 1995.
- [21] S. D. Apostolidis, P. C. Kapoutsis, A. C. Kapoutsis, and E. B. Kosmatopoulos, "Cooperative multi-UAV coverage mission planning platform for remote sensing applications," *Autonomous Robots*, vol. 46, no. 2, pp. 373–400, 2022.
- [22] K. Shah, G. Ballard, A. Schmidt, and M. Schwager, "Multidrone aerial surveys of penguin colonies in antarctica," *Science Robotics*, vol. 5, no. 47, p. eabc3000, 2020.
- [23] Y. Li, H. Chen, M. J. Er, and X. Wang, "Coverage path planning for UAVs based on enhanced exact cellular decomposition method," *Mechatronics*, vol. 21, no. 5, pp. 876–885, 2011.
- [24] I. Vandermeulen, R. Groß, and A. Kolling, "Turn-minimizing multirobot coverage," in *Proc. 2019 International Conference on Robotics and Automation (ICRA)*, 2019, pp. 1014–1020.
- [25] M. R. Silva, E. S. Souza, P. J. Alsina, D. L. Leite, M. R. Morais, D. S. Pereira, L. B. P. Nascimento, A. A. D. Medeiros, F. H. Cunha Junior, M. B. Nogueira *et al.*, "Performance evaluation of multi-UAV network applied to scanning rocket impact area," *Sensors*, vol. 19, no. 22, p. 4895, 2019.
- [26] L. Bauersfeld and D. Scaramuzza, "Range, endurance, and optimal speed estimates for multicopters," *IEEE Robotics and Automation Letters*, vol. 7, no. 2, pp. 2953–2960, 2022.
- [27] F. Nekovár, J. Faigl, and M. Saska, "Multi-tour set traveling salesman problem in planning power transmission line inspection," *IEEE Robotics and Automation Letters*, vol. 6, no. 4, pp. 6196–6203, 2021.
- [28] K. Shah, A. Schmidt, G. Ballard, and M. Schwager, "Large scale aerial multi-robot coverage path planning," *Field Robotics*, vol. 2, no. 1, 2022.
- [29] Y. Gabriely and E. Rimon, "Spanning-tree based coverage of continuous areas by a mobile robot," *Annals of Mathematics and Artificial Intelligence*, vol. 31, pp. 77–98, 2001.
- [30] Y. Zhang, Q. Wang, Y. Shen, T. Wang, N. Dai, and B. He, "Multi-AUV cooperative search method based on dynamic optimal coverage," *Ocean Engineering*, vol. 288, p. 116168, 2023.
- [31] R. Draves, J. Padhye, and B. Zill, "Routing in multi-radio, multi-hop wireless mesh networks," in *Proceedings of the 10th Annual International Conference on Mobile Computing and Networking (MobiCom '04)*. New York, NY, USA: Association for Computing Machinery, 2004, pp. 114–128.
- [32] "Ubiquiti bullet," <https://www.netwifworks.com/Bullet-M.asp>, accessed: Aug. 18, 2024.